April 2021

Jet Breakup Dynamics of Inkjet Printing Fluids

Kashyap Sundara Rajan
University of Massachusetts Amherst

Jet Breakup Dynamics of Inkjet Printing Fluids

Kashyap Sundara Rajan

JET BREAKUP DYNAMICS OF INKJET PRINTING FLUIDS

A Masters Thesis Presented

by

KASHYAP SUNDARA RAJAN

Submitted to the Graduate School of the
University of Massachusetts Amherst in partial fulfillment
of the requirements for the degree of

MASTER OF SCIENCE IN MECHANICAL ENGINEERING

February 2021

Mechanical and Industrial Engineering

JET BREAKUP DYNAMICS OF INKJET PRINTING FLUIDS

A Masters Thesis Presented

by

KASHYAP SUNDARA RAJAN

Approved as to style and content by:

_____
Jonathan P. Rothstein, Chair

_____
David P. Schmidt, Member

_____
Xian Du, Member

_____
Sundar Krishnamurty,
Department Head
Department of Mechanical and Industrial Engineering

ABSTRACT

JET BREAKUP DYNAMICS OF INKJET PRINTING FLUIDS

February 2021

KASHYAP SUNDARA RAJAN

B.Tech, Amrita Vishwa Vidyapeetham

M.S.M.E, University of Massachusetts Amherst

Directed by: Professor Jonathan P. Rothstein

Continuous InkJet (CIJ) printing is a common 2-Dimensional printing technique that creates jets of ink that breakup into drops as they are propelled towards a substrate to create a print. Inkjet printing has been used not only to print on paper, but to manufacture a variety of devices including OLEDs, solar cells and microfluidic devices. In many cases, the 'ink' consists of a polymer dissolved in a volatile solvent. As this ink is sprayed on to the substrate, the solvent evaporates, leaving the polymer behind as the print. The addition of the polymer alters the physics of the problem significantly enough that it varies greatly from jetting only a fluid with nothing dissolved in it. Polymers impart viscoelasticity to the solution, creating ink jets that are long-lived and difficult to break into droplets. In order to maintain the formation of drops in a repeatable, uniform fashion, a disturbance of known magnitude is imposed upon the jet. While jetting a liquid with no additives in it, this disturbance governed jet breakup leads to the formation of satellite drops, smaller drops of fluid in-between the main jet drops. Satellite drops are an undesirable occurrence in inkjet printing because of their unpredictable behavior and potential to affect the quality of the print. However, the addition of polymers to the liquid can control and potentially suppress

the formation of these satellite drops, greatly improving the print quality. The elasticity of the polymer and its ability to influence the jet behavior and formation of satellite drops is highly dependent on multiple factors including the backbone rigidity, molecular weight and the concentration in which it is present in the fluid. Strongly viscoelastic effects have a marked effect on the jet and their presence can be quantified quite easily. However, some polymers show weak viscoelastic behavior while present in the ink fluids and may or may not affect the jetting process. The objective of this study is to examine such a class of polymeric fluids that are weakly viscoelastic in the context of inkjet printing and satellite drop formation. Firstly, the fluids are tested in an extensional rheology setup called Capillary Breakup Extensional Rheometry – Drop-on-Substrate (CaBER-DoS) to quantify their extensional properties. Then, they are tested in an emulated inkjet printing setup. The goal is to quantify the impact of the aforementioned factors on jetting and using satellite drop behavior as a guiding metric to understanding viscoelastic behavior in inkjet printing fluids.

TABLE OF CONTENTS

LIST OF TABLES

LIST OF FIGURES

Figure Page

CHAPTER 1

INTRODUCTION

1.1 Non-Newtonian Fluids

Non-Newtonian fluids make up a significant portion of the fluids we encounter in our day-to-day-life. The main difference between a Newtonian and a Non-Newtonian fluid is that the Non-Newtonian fluid displays a non-linear response to a force exerted on it. This response may be in the form of a varying viscosity (the fluid thickens or thins in response to the applied force) or in the form of elasticity. This behavior of Non-Newtonian fluids arises from the physical components of the fluid in the form of dissolved high-molecular weight polymers or suspended micro/nano sized particles. A polymer molecule dissolved in a fluid exists in a coiled random equilibrium state. However, when the fluid is subjected to a deforming force, the coil is stretched out of its deformed state. A restoring, spring-like elastic force acts on the polymer, returning it to the earlier equilibrium state. The time taken for this returning process is characteristic of the polymer and is termed the relaxation time,

$$\lambda = \frac{\eta}{G} \tag{1.1}$$

Where λ is the relaxation time, η is the viscosity of the fluid and G is the elastic modulus of the polymer. It is also important to quantify if the elastic effects are apparent in the flow of the fluid. This is done using the Weissenberg number, described as,

$$Wi = \lambda\dot{\gamma} \tag{1.2}$$

Where Wi is the Weissenberg number, λ is the relaxation time and $\dot{\gamma}$ is the inverse of time scale of the flow. If $Wi \ll 1$, then the relaxation time is insignificant compared to the time scale of the flow, the polymer quickly returns to its equilibrium state and the elasticity effects are not apparent in the flow. However, if $Wi \gg 1$, then the time scale of the flow is comparable to the relaxation of the polymer and hence the elastic effects become apparent. [1,2]

Polymers are used in many places for different applications, including inkjet printing, coatings, agro-chemical sprays, and micro/nanoscale devices, paints, and in pharmaceutical applications. Hence, a thorough understanding of the behavior of each polymeric fluid both intrinsically and relative to their particular application is crucial to determining their efficacy for each application. An accurate, well rounded determination of the fluid properties in the respective flow conditions can shed light on how the fluids will behave in real-life conditions. Shear and extensional rheology are excellent starting tools to understand fluid properties because of the simplicity of the flow. They provide an insight into how the fluids react when subjected to shear and extensional flow, which form the basis of multiple complex flow problems.

1.2 Jet Breakup

Jet breakup is a classical problem in the field of fluid mechanics, dating back to the 19th century. It is a well-known phenomenon that a cylindrical jet of fluid decays into drops under the influence of surface tension. Experiments by Savart showed that

disturbances on the surface of fluid jets grew to break the jet into drops. Jet breakups occur independent of gravity, viscosity of the fluid, and the velocity and radius of the jet, and the instability that breaks the jet up originates from disturbances at the nozzle of the jet. Subsequently, Plateau[3] and Rayleigh[4] independently found that disturbances that resulted in a decrease in the surface area were favoured and grew because of surface tension. Rayleigh found that for the disturbance to grow on the jet, the wavelength of the disturbance had to be greater than the circumference of the jet, and the most unstable mode of disturbance corresponded to 1.4 times the jet circumference. [5] The time scale on which the jet break up occurs is $t_0 = \left(\frac{r^3\rho}{\gamma}\right)^{1/2}$ where ρ is the density of the fluid, γ is the surface tension and r is the jet radius. [6]

1.3 Inkjet printing

Figure 1.1 shows a sample inkjet printing setup, a 2D printing technique in which drops of ink are generated from a nozzle and propelled toward substrates to create an image. Inkjet printing has been used traditionally to print on paper and plastic based substrates, but increasingly has found use in the manufacture of multiple devices such as OLEDs, solar-cells and biosensors. [7–11] Figure 1.2 shows these devices produced with an inkjet printing process. There are two major categories – Drop-On-Demand (DOD) and Continuous InkJet (CIJ). DOD inkjet printing has a fluid reservoir connected to the nozzle and an actuation mechanism creates a rapid change in the volume of the reservoir that acts as a pulse to eject a specific quantity of ink through the nozzle. In CIJ, a continuous stream of ink is generated and broken into droplets by

an imposed regular disturbance. The droplets necessary for a print are directed toward a substrate, while the remainder is collected and reused. [12,13]

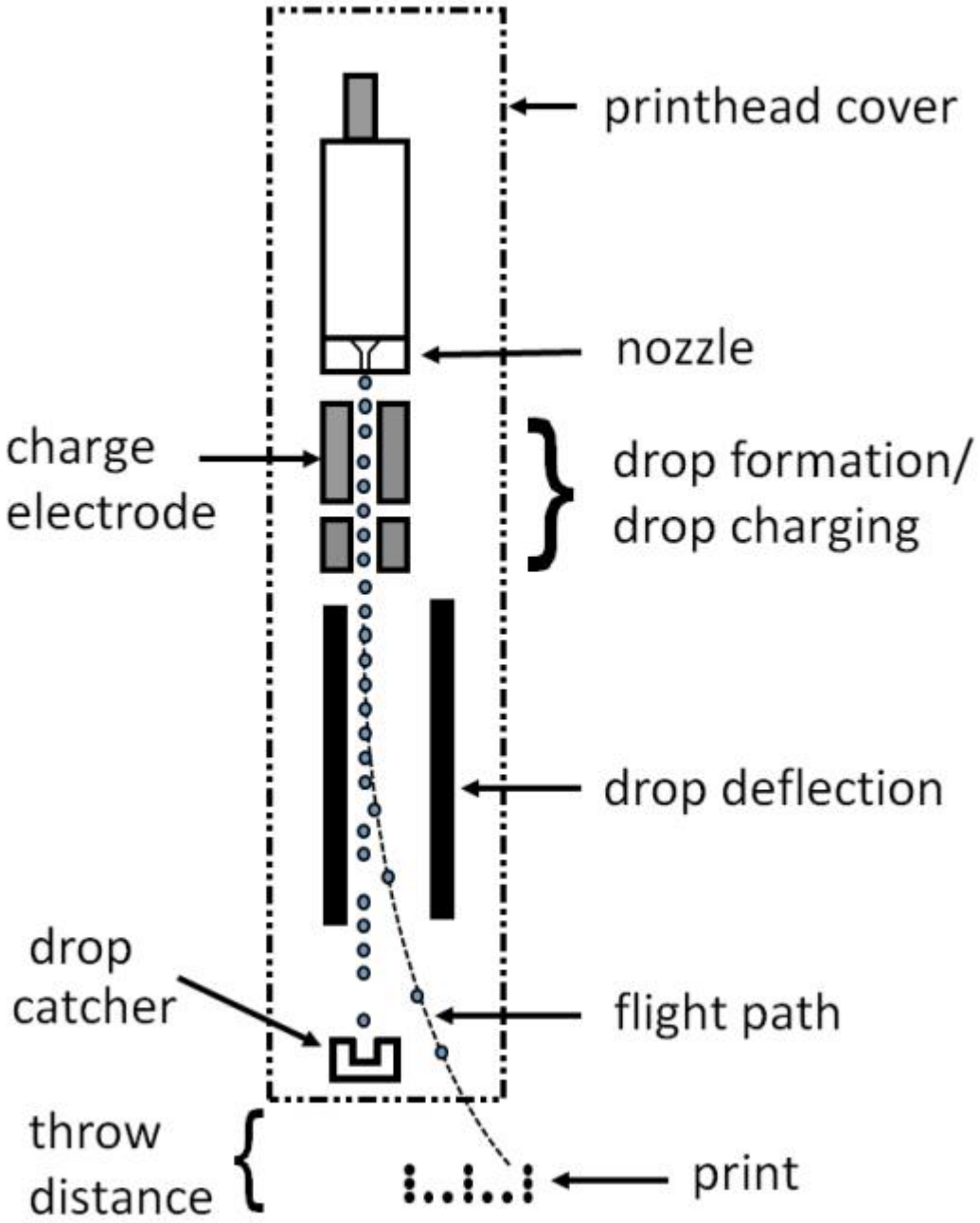

Figure 1.1: Sample Continuous InkJet Printing setup. [13]

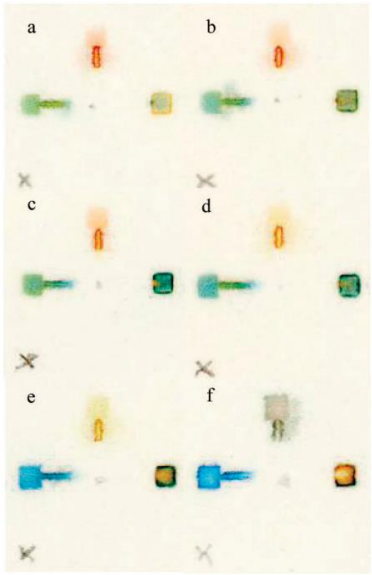

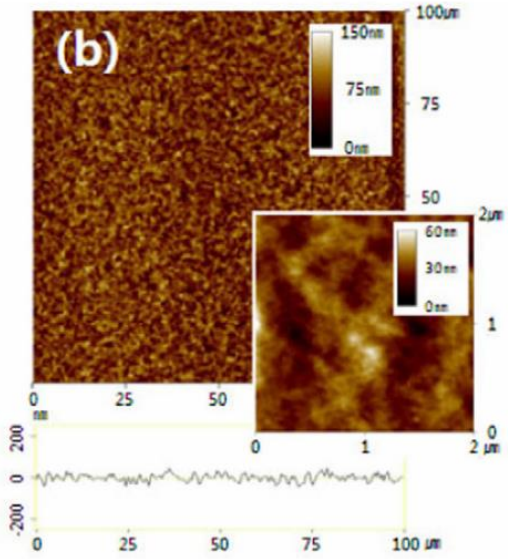

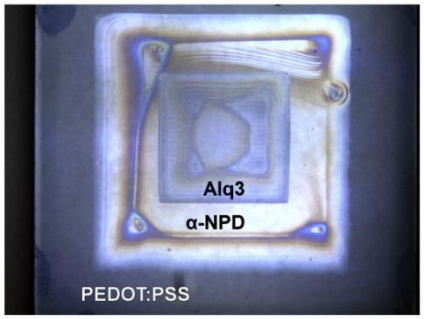

(a) **(b)** **(c)**

Figure 1.2: (a) Microfluidic Multianalyte system, [9] (b) AFM image of a solar cell [10] and (c) Organic Light Emitting Diodes [11] made using InkJet printing

1.4 Polymers in inkjet printing

Polymer addition to inkjet printing fluids is beneficial on many levels. Polymers allow the printing process to be executed with a greater degree of flexibility and accuracy and greatly increase the quality of the print. [14] In some cases, polymers are dissolved in a volatile solvent and the solution is used as an inkjet fluid. Upon deposition on the substrate, the volatile solvent evaporates, leaving the polymer behind as the print. Polymers can also be used for aesthetic purposes such as imparting colour to the print, instead of merely functional applications. Polymer properties uniquely affect the process of formation and the break-up of fluid jets. [14–17] Middleman mathematically modeled the growth of disturbances in a viscoelastic jet, under the assumptions of linear stability and a linear viscoelastic model. Under these conditions, a viscoelastic jet was found to be less stable than a Newtonian jet subjected to similar parameters. [18] Goldin et al continued the work, analyzing Newtonian, non-Newtonian inelastic, weakly viscoelastic and strongly viscoelastic fluids. Weakly viscoelastic and non-Newtonian inelastic fluids were shown to be less stable than idealized Newtonian fluids (with low jet velocities) and the breakup could also be modeled under linear stability analysis, which showed that the results are in good agreement with Middleman's work. [19] However, as the fluids became strongly viscoelastic, the non-linear effects increased, and the fluid formed droplets that were connected by fluid filaments. However, the droplets do not move uniformly, and they may move up or down the filaments and merge with other droplets. The filament bridge formed in between is of particular importance, because depending on the operating conditions, it

may either merge into the droplets, or it may detach from both its parent droplets, and form an independent droplet by itself known as a satellite droplet. [19] Entov and Yarin theorized that the slow disturbance growth in the later stages of jet breakup of a viscoelastic jet was due to elastic stresses arising from the dissolved macromolecules stretching and aligning themselves along the direction of the flow and also provided models to evaluate the stresses. [20]

1.5 Quantifying the different regimes of break up

Interplay of different factors govern jet break up and drop formation. At each point in time during the breakup, one factor dominates the break-up dynamics. These can be quantified using non-dimensional numbers, such as,

$$\text{Reynolds number, } Re = \frac{\rho v l}{\eta} \tag{1.3}$$

$$\text{Weber number, } We = \frac{v^2 \rho l}{\gamma} \tag{1.4}$$

$$\text{Ohnesorge number} = \frac{\sqrt{We}}{Re} = \frac{\eta}{\sqrt{\rho \sigma l}} \tag{1.5}$$

$$\text{Elasto-Capillary number, } Ec = \frac{\lambda \sigma}{\eta R} \tag{1.6}$$

Where ρ is the density, v is the velocity, γ is the surface tension, η is the dynamic viscosity, l is a characteristic length scale, λ is the relaxation time and σ is the surface tension.

The Ohnesorge number relates the effects of viscous forces to capillary forces. In a Newtonian or non-Newtonian inelastic fluid, Ohnesorge number can be used a measure for drop formation. If Oh <<1 the thinning dynamics are governed entirely by

inertial forces. If Oh>>1 the viscosity of the fluid dominates the break-up. The transition from the inertia-dominated break up to viscosity-dominated break up occurs at Oh = 0.2077. [21,22] For viscoelastic fluids, transitions occur at Ec > 4.7 from viscous-dominated to elasticity-dominated break up. In elastic fluids, Weissenberg number (Wi = $\dot{\epsilon}\lambda$) is an indicator of whether the elastic effects are significant. The jet forms drops connected by filaments that thin exponentially until the polymer chains become fully extended, and elasticity dominates the break-up. If Wi < ½, the chain has not deformed significantly enough to affect the flow and Newtonian mechanics can be used to model the fluid. However, if Wi > ½ the polymer chains extend and their presence affect the thinning dynamics. [23]

1.6 Quantifying fluid properties

Gaining a perspective on the fluid properties is an important start to any fluid problem. This is especially true in a problem like inkjet printing where minute changes in fluid composition drastically affects fluid properties, in turn influencing the flow itself. Extensional rheology is an important tool to understand fluid properties because inkjet printing itself is an extensional flow. There are two types of extensional rheology techniques – filament stretching and filament thinning techniques. [24] For the purpose of this study, filament thinning techniques are used more. In filament thinning, an unstable liquid bridge is formed between static end plates. This liquid bridge decays under the action of capillary forces. The thinning process is heavily influenced by fluid properties, and the influence of these properties can be measured by the non-dimensional numbers shown above. The bridge decay can be curve-fitted to obtain the properties of the fluid such as extensional viscosity and relaxation time. This technique

is formally called Capillary Breakup Extensional Rheometry (CaBER) and can be used to resolve relaxation times as low as 1 ms.[25,26] An extension of CaBER is called DoS-CaBER (Drop On Substrate CaBER) where a drop of fluid is dispensed from a nozzle on to a substrate placed at an appropriate height below to create an unstable liquid bridge that eventually decays under the action of capillary forces. [27,28] The prominent advantages of this technique are that it is fast and has been shown to detect relaxation times as low as 20 μs, which make it ideal to test inks that are weakly elastic and volatile. [29] DoS-CaBER is also extensively used in this research for this very reason.

1.7 Objective

The objective of this study is to study a class of commercially available inks in the context of a real inkjet printing setup. These inks are polymeric fluids with different polymeric binders which impart them different degrees of viscoelasticity. Multiple jetting studies, both numerically and experimentally have been carried out on fluids that are strongly viscoelastic. However, few studies exist on jetting weakly viscoelastic solutions, which will be the focus of this research work. The type and concentration of the polymeric binder can greatly influence the life of the filament in-between the drops, [30] and by extension, the formation and the size of the satellite drops.[31–33] Satellite drops are an undesirable occurrence in inkjet printing because they affect the quality and accuracy of the print. Hence, understanding the behavior and potentially elimination of satellite drops can greatly improve the quality of inkjet printing. Since satellite drops are formed by the filaments in-between the main drops, and these filaments are dependent on the elasticity of the polymeric binder used, it is useful to quantify the presence of elasticity in the flow. Too little elasticity can negatively affect the process

by allowing bigger satellite drops to form, while having no polymeric binder is undesirable from an industrial standpoint. On the other end, too much elasticity can also negatively affect the inkjet printing process having filaments that are sustained long enough for the main drops to merge into themselves. [34]

Previously conducted studies on the fluids used in this study used an extensional rheology technique called Dos-CaBER (Drop-On-Substrate Capillary Breakup Extensional Rheometry) to analyze the modes of break up in the fluid flow. Rosello et al identified the dominant mode of break up (inertial, viscous or elastic) at each point in time of the flow, and provided a mathematical model to predict the mode that dominated the thinning dynamics of the flow. [35] This research aims to extend Rosello's study further, by testing the fluids in a real inkjet printing setup. The objective of this research study is twofold. Firstly, can the mode of break-up of different weakly viscoelastic polymeric fluids in an inkjet printing be identified? If so, what will the deciding metric be to demarcate the modes? Secondly, to emulate real-life inks, microparticles are added to the solutions. How will the presence of microparticles affect the weakly viscoelastic nature of the inks and the jetting process in general?

CHAPTER 2

EXPERIMENTAL METHODS

2.1 Jetting setup

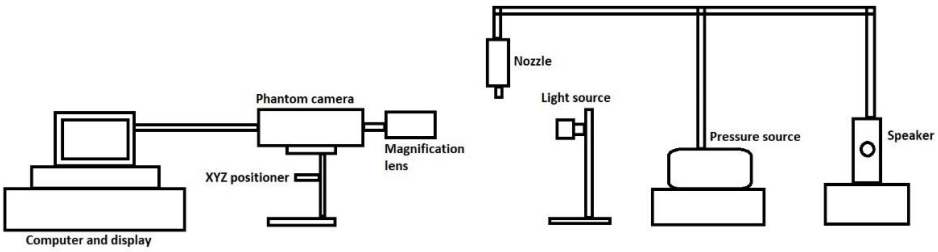

Figure 2.1: A schematic of the jetting setup and data acquisition system used in the experiments

A typical jetting setup used is shown above. A nozzle of diameter 800 um with a fluid reservoir is connected to a pressure source and speaker. The pressure source drives the fluid out of the reservoir through the nozzle at pressures of 4-6 psi (depending on the polymer used), while the speaker imposes a frequency of 800 Hz on the fluid to enable the break-up. The pressure and frequency are calibrated to ensure the growth of the maximum disturbance mode. A 5x4 light array illuminates the jet. A high-speed camera (Phantom Vision V4.2) with a Nikon 18-55mm lens is used to capture the break-up at 10000-12000 frames per second (depending on the polymer used), within a window of 400x100 pixels. This setup was inspired by Donnelly and Glaberson's jet breakup study. [36]

2.2 Measurement methods

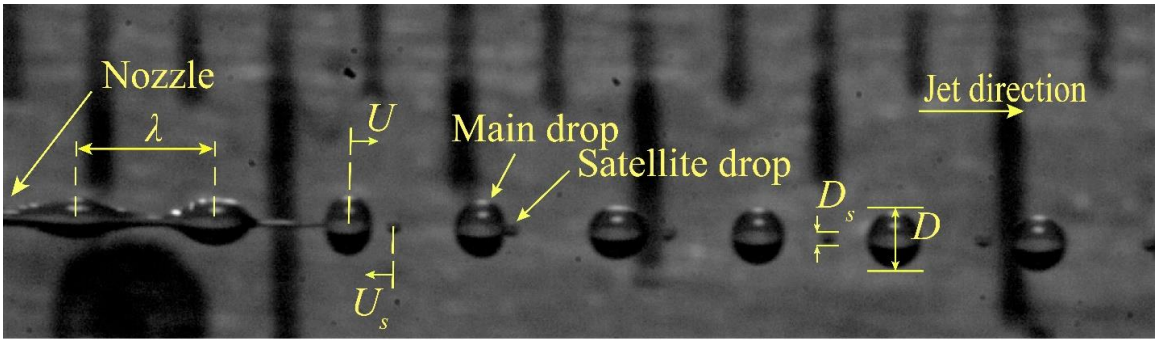

Figure 2.2: Sample measurements made on a jet break up

The above image is a sample measurement performed on the jet. The wavelength is defined as the distance between successive peaks on the jet, and is maintained between 2.13-2.4 mm (acceptable range for the growth of maximum disturbance). A ruler with $1/16^{th}$ inch demarcations is positioned in the background to help quantify distances. The velocity of the jet, U, is defined as the distance moved by a jet drop in a specified number of frames. With the frame rate per second established, this allows us to measure the speed of the jet. The velocity of the satellite drop, U_s, is defined as the distance moved by the satellite drop after becoming completely spherical and before colliding with the drops of the jet, in a specified number of frames. The diameter of the jet drop and the satellite drop are measured across the drops. The break-up distance is defined as the point at which a jet drop completely detaches from the jet. The break-up time is estimated from knowledge of the break-up distance and the jet velocity. From Rayleigh's theory, the most unstable breakup mode corresponds to a disturbance wavelength equal to 1.4 times the circumference of the jet. Based on the nozzle of diameter 800 μm, the wavelength

corresponds to 2.07 mm. However, taking experimental variation into account, the wavelength is maintained between 2.07 mm and 2.4 mm.

2.3 Capillary Breakup Extensional Rheometry – Drop On Substrate

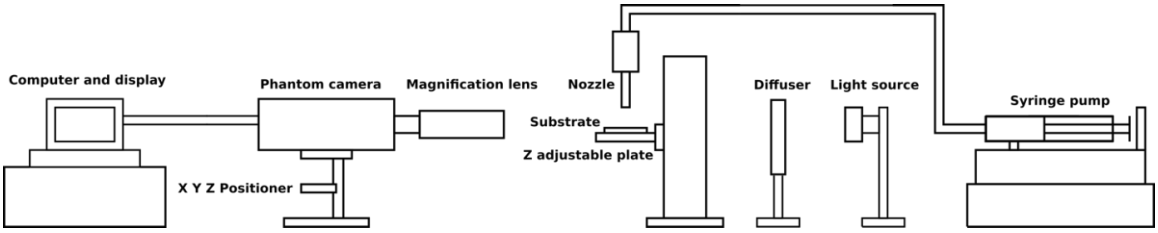

Figure 2.3: A schematic of a CaBER-DoS setup and data acquisition system

DoS-CaBER is the extensional rheology technique used in this study. In a DoS-CaBER setup, a fluid drop is formed through a nozzle using a syringe pump. The nozzle is suspended over a glass substrate at height, H = 1.6 cm. The drop is allowed to fall and spread onto the substrate only under the action of gravity. The Phantom high-speed camera is used to capture the breakup of the filament formed between the nozzle and the substrate at a frame rate of 20000-25000 frames per second in a window of 128x128 pixels. A microscopic lens attachment to the camera provides a magnification of 5μm per pixel. The diameter decay is digitized over time and measured using a software called Edgehog (courtesy of researchers at KU Leuven). The diameter decay data over time can be fitted using different equations to obtain the properties of the fluid. The three regimes of break up are inertial, viscous and elastic and their respective equations are provided below.

In an inertial diameter decay (low viscosity fluids), the thinning dynamics are governed by the interplay between inertial and capillary forces, and the filament decay follows a 2/3rd power law, [22,37]

$$\frac{R(t)}{R_0} = 0.64 * \left(\frac{\sigma}{\rho R_0^3}\right) * (t_c - t)^{2/3} = 0.64 * \left(\frac{t_c - t}{t_R}\right)^{2/3} \quad (1)$$

Where t_c is the breakup time of the filament and $t_R = \sqrt{\rho R_0^3 / \sigma}$ is the Rayleigh time, a characteristic timescale of fluids in the inertio-capillary regime. The 0.64 prefactor in equation 1 has been reported as being between 0.64 and 0.8. [28,38,39]

As the viscosity of the fluid increases, the fluid transitions to a viscous dominated breakup and the filament thinning is governed by the interplay between viscous and capillary forces. [40] The diameter decay then is linear:

$$\frac{R(t)}{R_0} = 0.0709 * \left(\frac{\sigma}{\eta_0 R_0}\right) * (t_c - t) = 0.0709 * \left(\frac{t_c - t}{t_v}\right) \quad (2)$$

Where $t_v = \eta_0 R_0 / \sigma$ is the timescale characteristic of a viscous break up . The transition between an inertia-capillary break up and a viscous-capillary breakup has been shown to occur at an Ohnesorge number of Oh = 0.2077 by Clasen et al. [22]

When elastic effects are apparent in the fluid, the elastic thinning regime is also present in the diameter decay. The filament first thins faster than a corresponding filament comprised only of a Newtonian fluid, but after elastic effects become apparent, the filament either thins slowly or is sustained. [41] The fluid filament thinning can be described using a FENE-P model.

$$\frac{R(t)}{R_0} = \left(\frac{GR_0}{2\sigma}\right)^{1/3} * e^{-t/3\lambda_E} \quad (3)$$

Where G is the elastic modulus of the polymer, λ_E is the relaxation time of the polymer. The transition from an inertia-capillary break up to an elastic-capillary breakup happens at Deborah number, De > 0.98 and a transition between viscous-capillary and elastic-capillary thinning happens above an elasto-capillary number of Ec > 4.7.

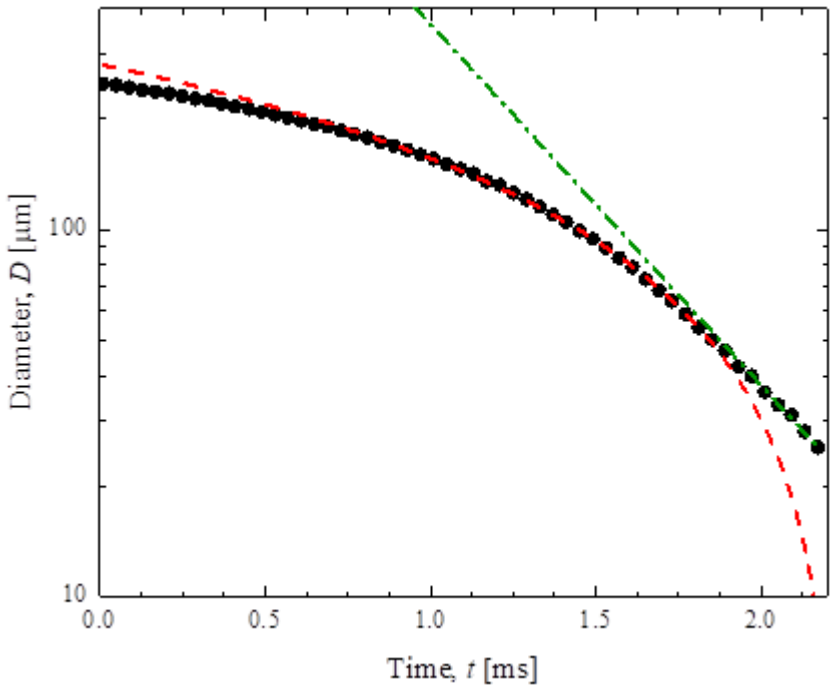

Figure 2.4: Sample diameter decay using CaBER-DoS versus time for a weakly elastic fluid with two fits: viscous (- -) , fitted using Equation 2 and elastic (- · -), fitted using Equation 3. [35]

2.4 Fluid Rheology

This research was carried out on two sets of polymeric binders: CAB-381-2 (Eastman chemicals) also known as Cellulose Acetate Butyrate, a cellulose based polymer, and Vinnol E22/48A (Wacker Chemie), a vinyl based co-polymer. The properties of the polymers are listed in Table 1. The solvent for both binders was Methyl Ethyl Ketone (MEK), having a zero-shear viscosity of η_s = 0.43 mPa-s and a surface tension with air of σ = 24 mN/m at 20°C. The density of the solutions were also found to be the same as that of MEK, ρ = 865 kg/m^3. [35,42] Owing to spatial resolutions in the data acquisition system, some relaxation times cannot be measured accurately and are reported as null values.

The polymer properties are presented in the table below:

Table 2.1: List of polymeric binders used in the inkjet experiment and their properties. [35]

Binder name	Chemical Nature	M_n [g/mol]	M_w [g/mol]	Polydispersity Index	c^* [wt%]
Cab-381-2	Cellulose	52900	158900	3.0	1.4
Vinnol E22/48A	Vinyl Chloride	37800	118300	3.1	3.2
Vinnol E15/45M	Vinyl Chloride	28900	67700	2.3	3.7
Paraloid B66	Acrylic	27300	51800	1.9	6.8

Table 2.2: A list of the concentrations used in this study along with their respective zero shear viscosities (measured in a couette rheometer) and extensional relaxation time [35]

CAB-381-2		
Concentration [wt%]	η_0 [mPa.s]	λ_E [μs]
4	6.9	-
5	9.4	-
6	16.9	71
Vinnol E22/48A		
6	6.0	740
7	6.7	815
8	8.1	1000
Vinnol E15/45M		
8	3.5	-
12	7.9	-
14	12	-
16	17.5	78
17	20.4	275
Paraloid B66		
15	5	-
20	6.9	-
25	13.3	-
30	25	140

CHAPTER 3

RESULTS

3.1 Break up time

Break up time is defined as the break-up distance divided by the velocity of the jet. Break up time is an excellent indicator of the different regimes present in the fluids. As the perturbations in the fluid jet become significant and the effects of surface tension are apparent, the peaks of the perturbations coalesce into the jet drops, separated by long, thin cylindrical filaments. These filaments eventually break off and condense into satellite drops, in between the drops of the jet. When the concentration of the polymeric binder is low, the effects of elasticity are not apparent in the fluid jet. However, upon increasing the concentration of the polymer, especially in CAB, the fluid transitions from being inelastic to being weakly elastic. This effect is seen in the break-up time, which increases as the effect of elasticity are felt. In the other Vinnol E22/48A case, as the effect of elasticity increases, the break-up time also increases. Hence a direct correlation can be observed between the presence of elasticity and increase in break up time. In the later stages of the filament breakup, the breakup process transitions from being inertia dominated to being viscosity dominated, and as the concentration increases, elasticity dominated. As seen in CaBER-DoS, viscous filaments decay slower than inertial filaments do, and elastic filaments decay slower than viscous filaments do. [34] This is also correspondingly reflected in the breakup of the Vinnol E15/45M and the Paraloid B66, the other two polymeric binders used in the study. The Paraloid data is the work of undergraduate student Samantha Bonica, who was also a member of the NNFD lab. A sharp increase in the breakup time

was observed in the Vinnol E15 binder at the 17 wt% concentration, as the elastic effects became apparent. As this binder is quite sensitive to concentration effects, it shows this trend. The Paraloid, which shows an elastic response only at the 30 wt% case, did not show a sharp response, but rather a continued increase in breakup time with the increase in concentration. Hence, viscosity in by itself proves to be a factor to slow down the growth of perturbations and increase the breakup time, but at specific concentrations, the effects of elasticity become apparent, and elasticity further delays the breakup of the filaments formed in-between the drops, thereby increasing the breakup time.

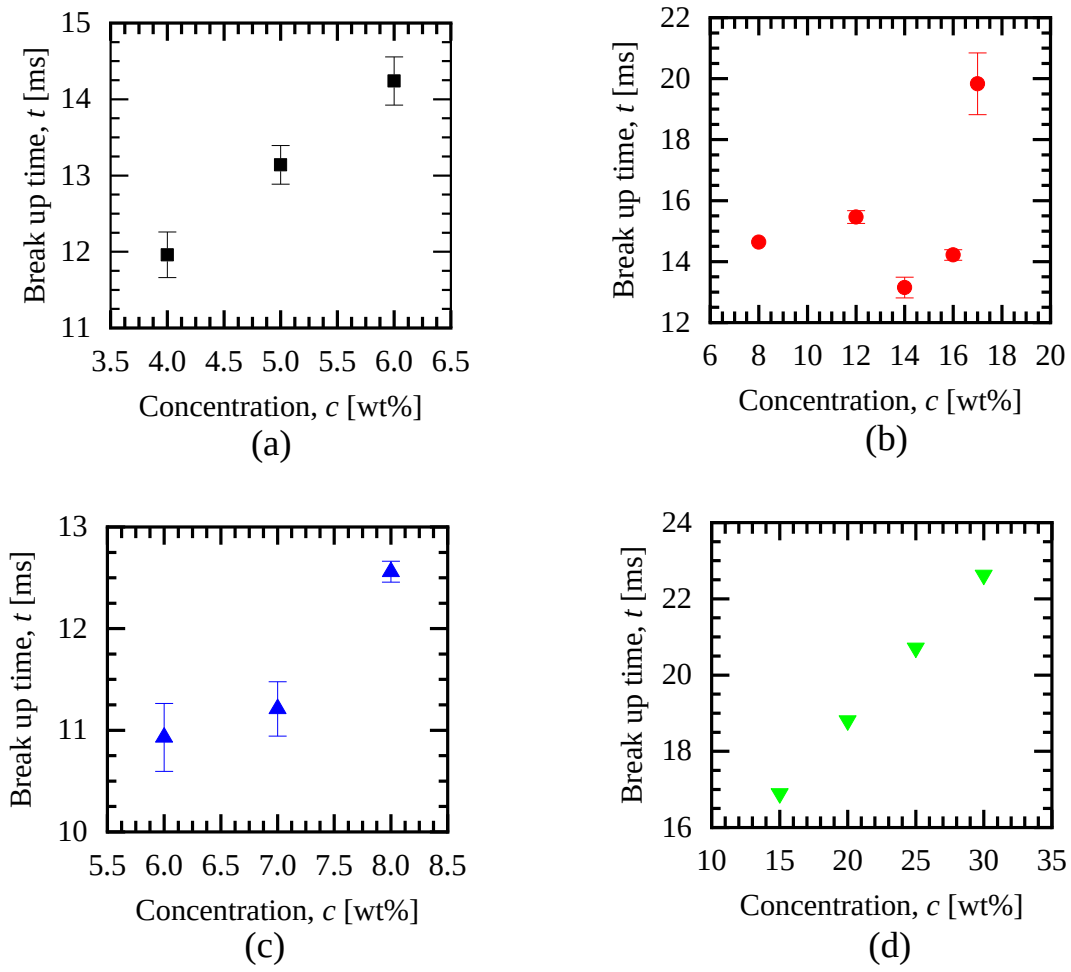

Figure 3.1: Variation of break up time with concentration for (a) CAB and (b) Vinnol E15/45M (c) Vinnol E22/48A and (d) Paraloid B66

3.2 Main drop volume

As the fluid transitions from having a completely inertial jet to being mildly viscoelastic, the effects of such a transition can be observed in the main drops. As seen in Figure 3.2, main drop volume is plotted as a function of concentration. For CAB, jet drop volume steadily increased as the concentration of polymer went up. Vinnol E22/48A was more responsive to the effects of elasticity, also showing an increase in main drop volume as the concentration of the polymer in the solution went up. This rise in main drop volume, which is a favourable occurrence, can be directly attributed to the effect of elasticity in the flow. Elasticity causes the 'trough' filaments in between the main drops to be exist longer, hence allowing the filaments to be sustained further as the fluid from the filaments drains into the two main drops. As the main drop volume increases, correspondingly, the satellite drop volume decreases, which is generally favourable in inkjet printing. Fluids can have lesser amounts of elasticity affecting drop formation, but the 6 wt% case for CAB was the limit of elasticity that was observed and quantified by extensional rheology measurements, and again observed in the jetting process. Both CAB and Vinnol show nearly similar values of main drop volume at the same concentration, 6%, and both are elastic at that concentration, suggesting that the elasticity, though different in magnitude for both the polymers, is enough to sustain the filament long enough for the filament to drain fluid back into the main drops. Hence, even the smallest amount of elasticity, as seen in the CAB with 71 μs relaxation time is enough to sustain the filament long enough for bigger main drops to form. [43,44] Similarly, Vinnol E15/45M shows comparable results for the main drop volume for the 8 wt%, 12 wt% and 14 wt% cases. However, with the system becoming

elastic at 16 wt% with a relaxation time of 78 μs, the main drop volume increases considerably. Similarly, the Paraloid B66 also shows an increase in main drop volume at 30 wt%, which is where the elasticity effects become apparent. This is a corollary to the results shown in the breakup time plots.

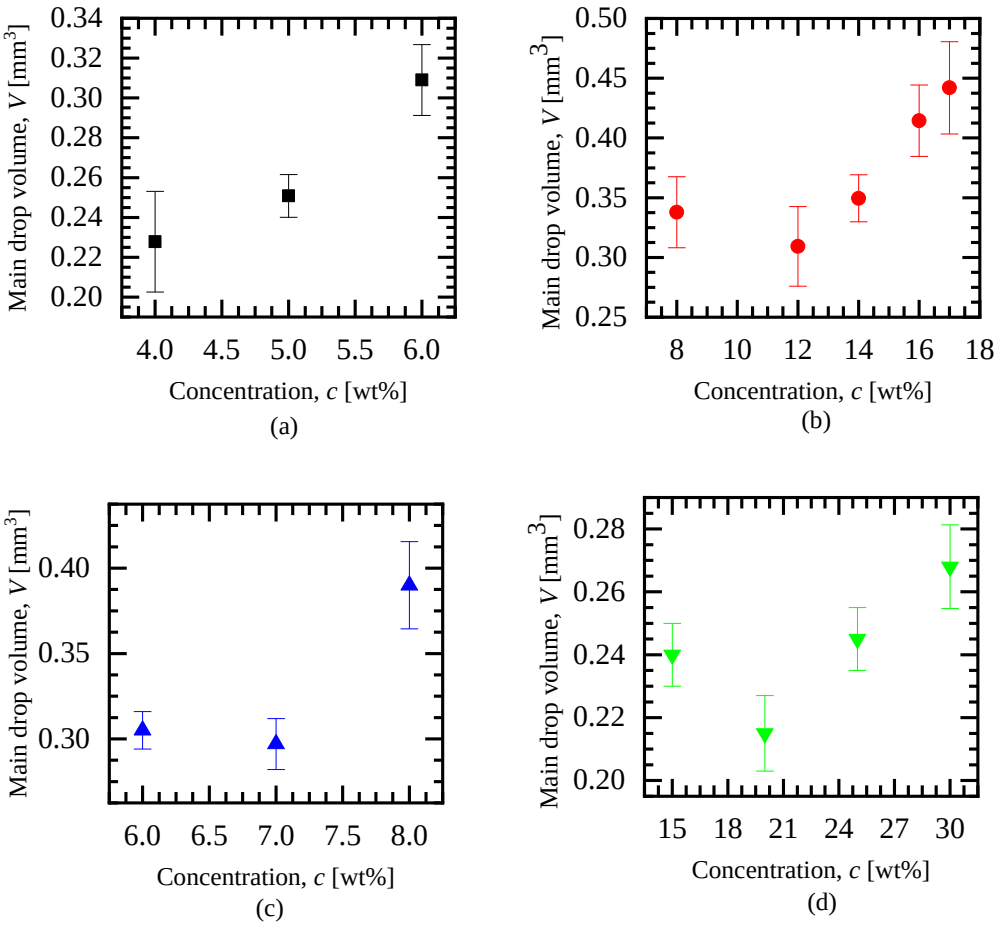

Figure 3.2: Variation of jet drop volume with concentration for (a) CAB and (b) Vinnol 15/45M (c) Vinnol E22/48A and (d) Paraloid B66

3.3 Analysis with relaxation time and shear viscosity

In figure 3.3, the breakup time is presented as a function of relaxation time and shear viscosity. CAB initially shows a completely inertial breakup at 4% where the filament forms a conical tip with the jet drop. Upon increasing the concentration to 5%, it shows an extended conical shape, characteristic of a viscous breakup, and finally at 6%, it forms extended, thin, cylindrical filaments that indicate the presence of elasticity in the flow. However, the Vinnol E22/48A is already highly elastic at 6%, and only shows increases in its elastic behavior as the concentration increases. Both CAB and Vinnol E22/48A are elastic at 6% concentration, but the CAB has a relaxation time which is an order of magnitude lesser than that of Vinnol. Although CAB has a higher molecular weight as compared to the Vinnol, the lower relaxation time results from the fact that CAB has a rigid backbone as a cellulose based polymer. [45] This is also reflected in the shear viscosity, as CAB and Vinnol at 6% show significantly different shear viscosities. Rosello et al [35] showed that elastic behavior in the fluid can be observed in a jetting setup, but such observance is highly dependent on both the relaxation time and shear viscosity. Vinnol E15/45M and Paraloid B66 are however, more sensitive to the effects of elasticity than CAB and Vinnol E22/48A. As seen in figure 3.4, another measure of elasticity is the behaviour of satellite drops or the drops forms by the coalescence of the in-between filaments. As the in-between filament separates from the jet and coalesces into a satellite drop, it moves with a speed that is dependent on the relaxation time and the elastic restoring force of the polymer. Since the satellite drop moves relative to the jet, its velocity is also measured in relation to the jet velocity. As the satellite drop detaches from the jet, the

elastic restoring force seeks to pull it back into the jet, and hence this trend of a negative satellite drop velocity is seen. Vinnol E15/45M and Paraloid B66 show significant, marked satellite drop behaviour in the presence of elasticity. With the slightest onset of elasticity, the satellite drop velocity becomes more negative, suggesting the action of a strong elastic restoring force on the satellite drops. Visualizing the satellite drop velocity as a function of relaxation time in figure 3.4, we see that the onset of elasticity can be directly corroborated with satellite drop behaviour. Hence, while CaBER-DoS is a versatile and powerful technique to understand the different regimes of breakup, satellite drop velocity is a rough yardstick to gauge the effects of elasticity in the flow. Vinnol E15/45M and Paraloid B66 are especially significant because of the ability to observe satellite drop behaviour in concentrations before and after the critical concentrations required for elastic behaviour. Therefore, since these effects are prominent, it is worthwhile to study the formation and motion of satellite drops in further detail and estimate the magnitude of these restoring elastic forces. This forms the basis of a future set of experiments or the satellite drop study.

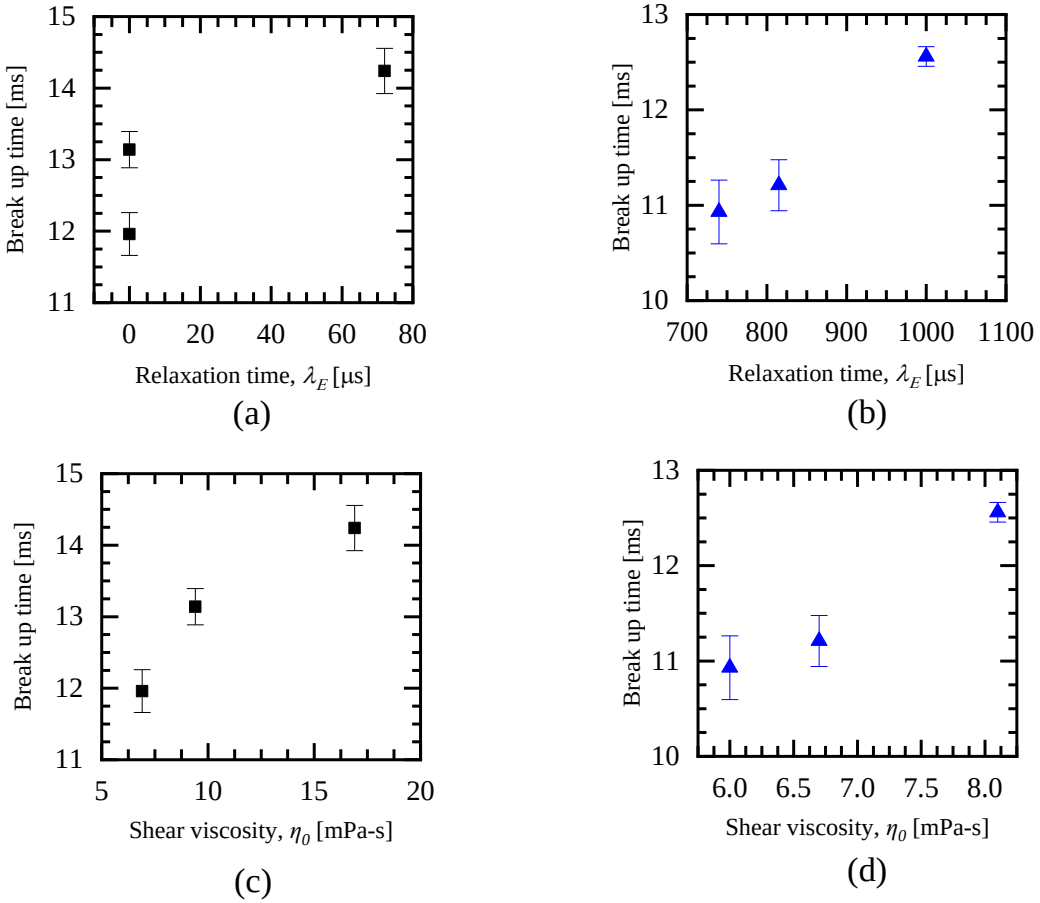

Figure 3.3: Variation of breakup time with relaxation time for (a) CAB and (b) Vinnol E22/48A and variation of breakup time with shear viscosity for (c) CAB and (d) Vinnol E22/48A

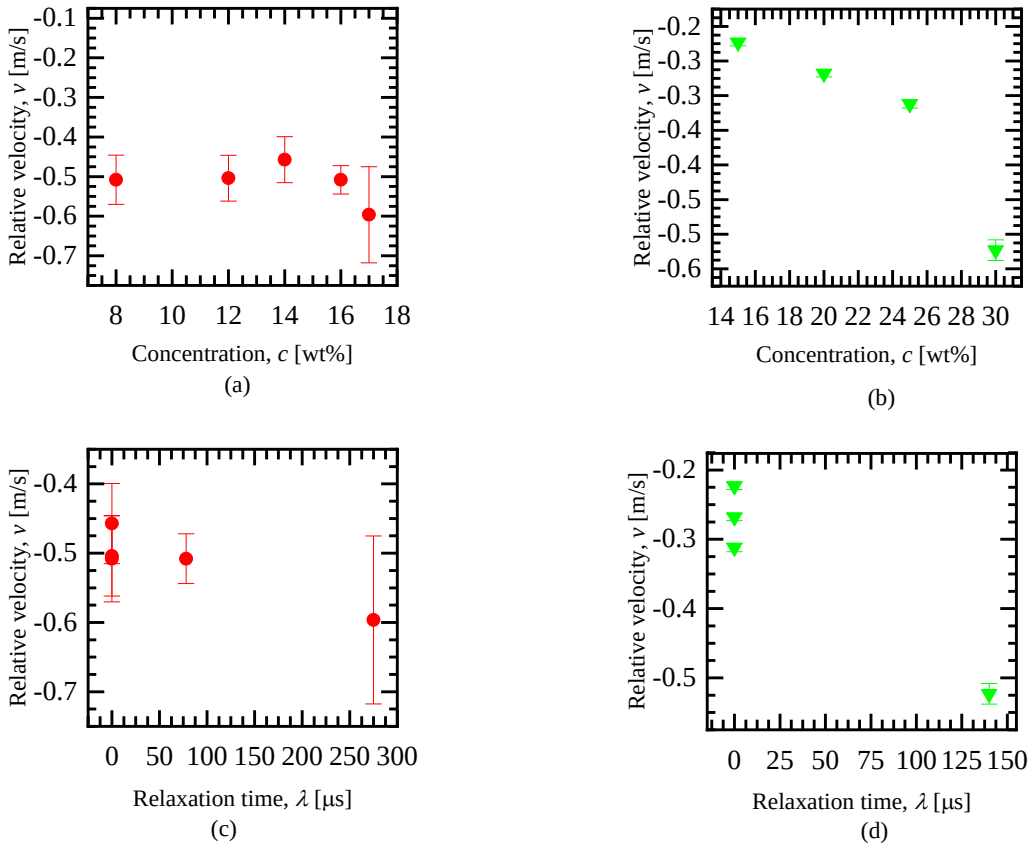

Figure 3.4: Variation of satellite drop retraction velocity with concentration for (a) Vinnol E15/45M and (b) Paraloid B66 and variation of satellite drop retraction velocity with relaxation time for (c) Vinnol E15/45M and (d) Paraloid B66

3.4 Theoretical predictions versus experimental results

In order to correlate the experiments with theory, the experimental results are compared to the theoretical modelling presented in Rosello et al's paper. The discussion in the paper includes a theoretical prediction of breakup time for the same fluids in a CaBER-DoS setup [35] and in this thesis, those predictions are extended to the jetting results. The prediction involves a theoretical transition radius as the fluid changes from an inertia-dominated to viscosity dominated breakup and also a prediction for the theoretical breakup time of the filament. These formulae are as follows:

$$R_t = 45.8\frac{\eta^2}{\rho\sigma} \tag{1}$$

$$t_b = \sqrt{\frac{\rho}{0.26\sigma}}\left({R_0}^{3/2} - {R_t}^{3/2}\right) + \frac{R_t\eta}{0.0709\sigma} \tag{2}$$

Where R_t is the transition radius and R_0 is the initial radius. This equation is obtained by manipulating equations (1) and (2). Values of shear viscosity, density and surface tension are substituted in this equation for various binders and the data is adjusted to allow for the growth of the perturbations on the jet. The results are presented in figure 3.5. As can be seen, the theoretical predictions do a reasonably good job of predicting the breakup time for low viscosity and inelastic fluids with small deviations owing to differences in the CaBER data curve fits. However, as we approach the cases where there are high shear viscosities coupled with elastic behavior like the 17 wt% Vinnol E15 and the 30 wt% Paraloid B66, larger deviations from the predicted behaviour is seen. This is another

indicator of the role elasticity plays in the breakup time, and hence, further investigation into the breakup process, particularly in the last few milliseconds of breakup can greatly help explain the elastic behaviour of the fluids. Similar analyses can be attempted for a transition from a viscosity dominted to an elasticity dominated breakup, but the breakup curve fits have two unknows – viscosity and relaxation time, both of which are obtained from the experiments and hence doing a similar analysis would require making assumptions about the fluid properties. This further reinforces the arguments in made in Section 3.3 and shows how elasticity, even if present in small quantities, can greatly affect the breakup process if the concentration of the polymeric binder is above the critical concentration, how the concentration of the binder causes an increase in shear viscosity of the fluid, which is reflected in the time required for the nucleation of the perturbations on the surface of the jets and how these two phenomenons are related. Hence, two sets of future experiments can be planned from these results. One – to study the breakup process in further detail, particularly in the higher concentrations of Vinnol E15/45M and Paraloid B66. Two – study the effect of particle addition in the viscosification of the solutions and breakup time trends. Vinnol E15/45M is chosen as the ideal candidate to continue the experiments with because of its ease of procurement.

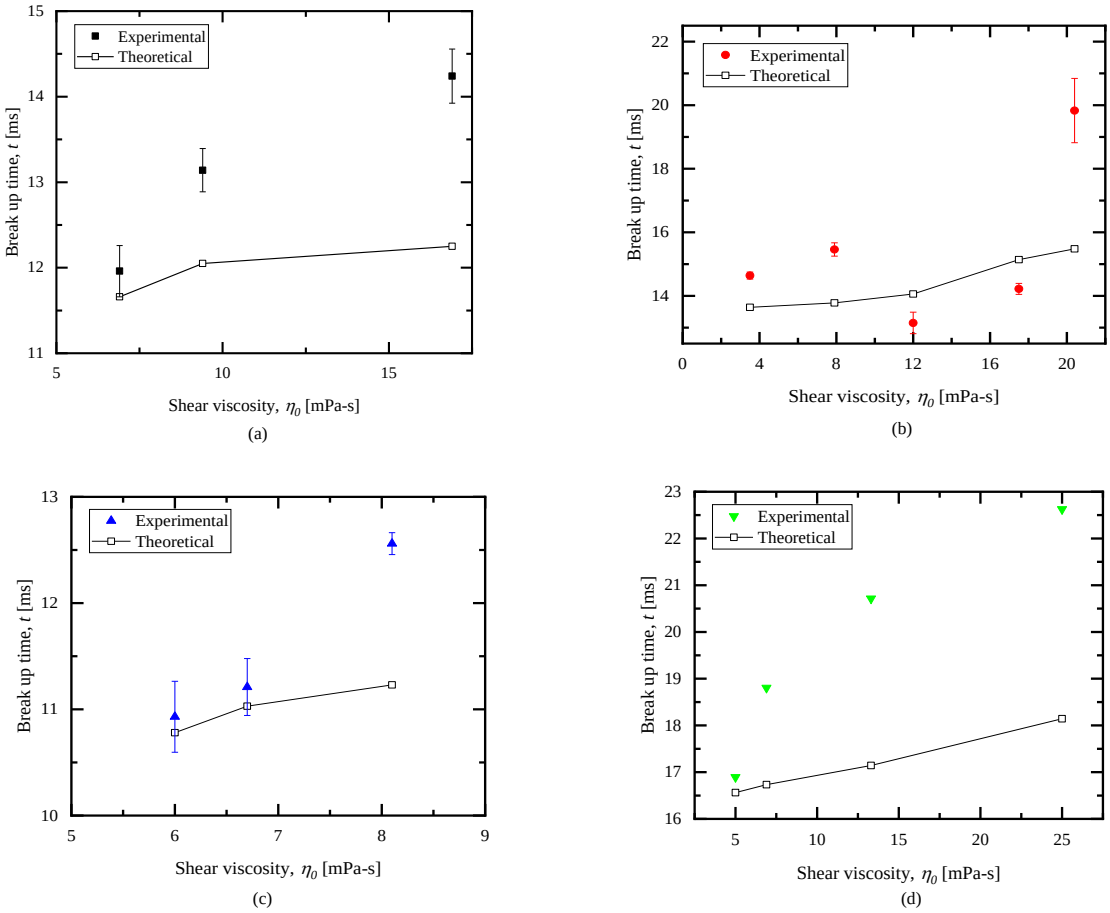

Figure 3.5: Theoretical breakup time and experimental results versus shear viscosity for (a) CAB (b) Vinnol E15, (c) Vinnol E22 and (d) Paraloid B66. The theoretical data is represented by hollow squares and lines whereas the experimental data is represented by data points.

3.5 Particle laden solutions – CaBER-DoS results

The third and final part of this thesis focuses on studying jetting results of particle laden solutions. Since Vinnol E15 showed the most sensitivity to the jetting process, it was again chosen as the ideal candidate to continue these jetting experiments with. However, since the lab supply of Vinnol E15 was not sufficient to generate all solutions, a new sample of Vinnol E15/45M powder was obtained from Wacker Chemie. This new batch of Vinnol E15/45M has rheological properties that are different from the previous batch used, hence new measurements had to be carried out. Vinnol E15 was mixed along with 8 μm SiO_2 particles in Methyl Ethyl Ketone to create the particle laden solutions. The Vinnol concentration was maintained at 16 wt%, whereas the microparticle concencentration was at 0 wt%, 0.5 wt%, 1 wt%, 2 wt% and 4 wt%. CaBER-DoS and jetting experiments were performed on all 5 samples. The final images from the breakup are shown in Figure 3.6. It was previously assumed that the 16wt% Vinnol with no particle addition would yield similar results to the 16 wt% Vinnol previously tested, but however that assumption was disproved through CaBER-DoS results. Hence, these results are treated as independent results with no correlation to the previous jetting results.

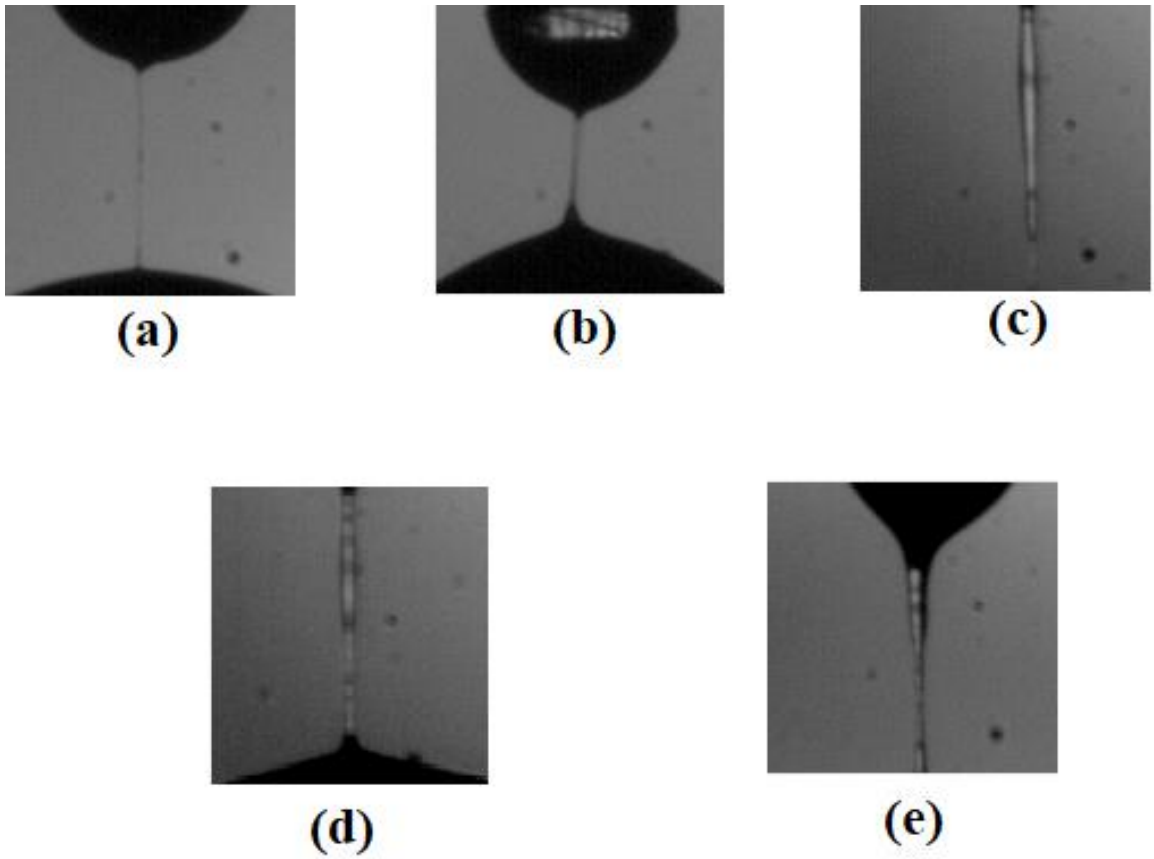

Figure 3.6: CaBER-DoS breakup images for 16 wt% Vinnol E15 with (a) 0 wt% SiO_2 (b) 0.5 wt% SiO_2 (c) 1 wt% SiO_2 (d) 2 wt% SiO_2 (e) 4 wt% SiO_2

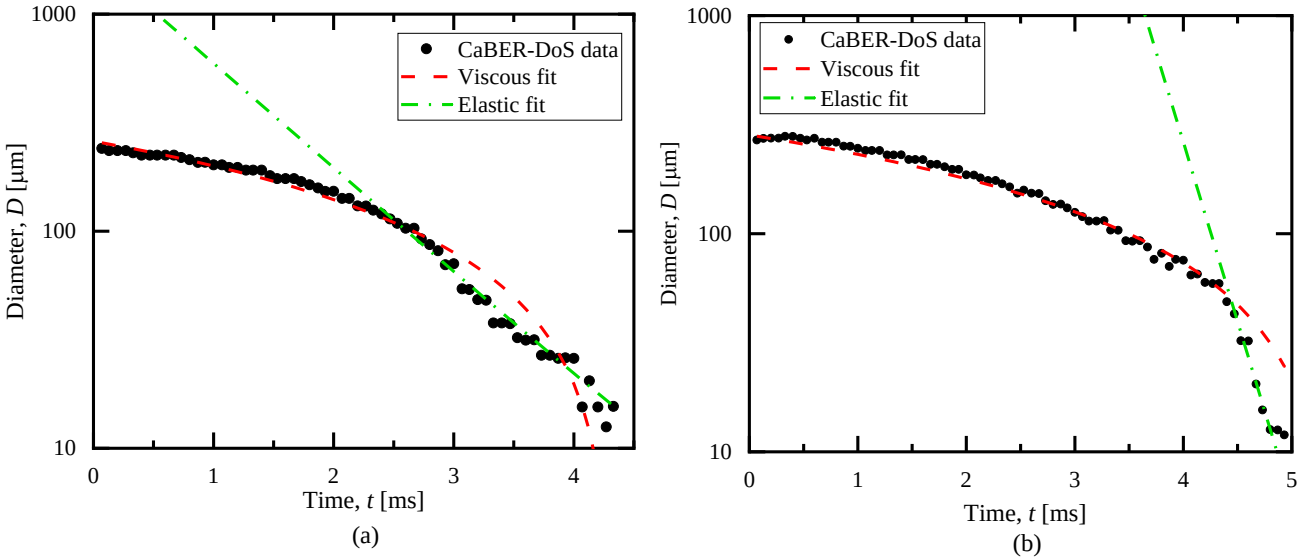

Figure 3.7: CaBER-DoS data and curve fits for 16 wt% Vinnol E15 with (a) 0 wt% SiO_2 (b) 1 wt% SiO_2

CaBER – DoS analysis of the 5 solutions yielded a multitude of results. Some sample CaBER – DoS data and the corresponding curve fits are shown in Figure 3.7. It can be observed from the breakup images and the data in Figure 3.7 that the region of validity of the elastic fit decreases with increase in concentration of the polymer, that is, fewer data can be represented by the elasto-capillary diameter thinning equation. Correspondingly, with the increase in concentration of the polymer, the region of the data represented by the viscous thinning equation increases.[46,47] This can also be seen in Figure 3.8, as the relaxation time of the solution with no particle addition is about 300 μs, and a viscosity of 12 mPa-s, whereas at 4 wt% concentration of the microparticles, the relaxation time is absent (the solution displays no elastic behaviour), but the viscosity of the solution increases to 28 mPa-s. As a consequence of this increased viscous behaviour, it becomes increasingly harder to produce consistent jets with particle laden solutions, with the 4 wt% microparticle solution providing an inconsistent jet that is not suitable for analysis. Another observance from the breakup images and the CaBER-DoS data is the presence of non-uniformity in the breakup of the solutions, as the concentration of the microparticles increases. This is likely due to non-uniform distribution of microparticles in the solution, and while efforts are taken to mitigate this occurrence, it cannot be completely eliminated, and this effect cascades into the results of jetting as well. Viscosity dominates the thinning dynamics for a significant part of the CaBER-DoS experiment. While the entire filament thins uniformly in a CaBER experiment with no particles added, CaBER filaments in solutions with particles added thin non-uniformly. The thinning happening in the filament is localized, and is in a region of the fluid which is locally deficient in the particles. The thinning dynamics, then, in the particle deficient region, depend solely on the properties of

the base fluid-polymer solution. The difference in viscosity of the polymer solution and polymer-particle solution becomes significant as the concentration of the polymer increases. With the increase in particle concentration in the solution, the polymeric binder gets adsorbed onto the surface of the particles. This results in the elasticity effects being suppressed with the increase in polymer concentration and the elastic behaviour of the fluid dominates the filament breakup less. This can be seen in the relaxation time graph, as the relaxation time is not sensed in the CaBER experiment with the 4 wt% particle solution. [48,49]

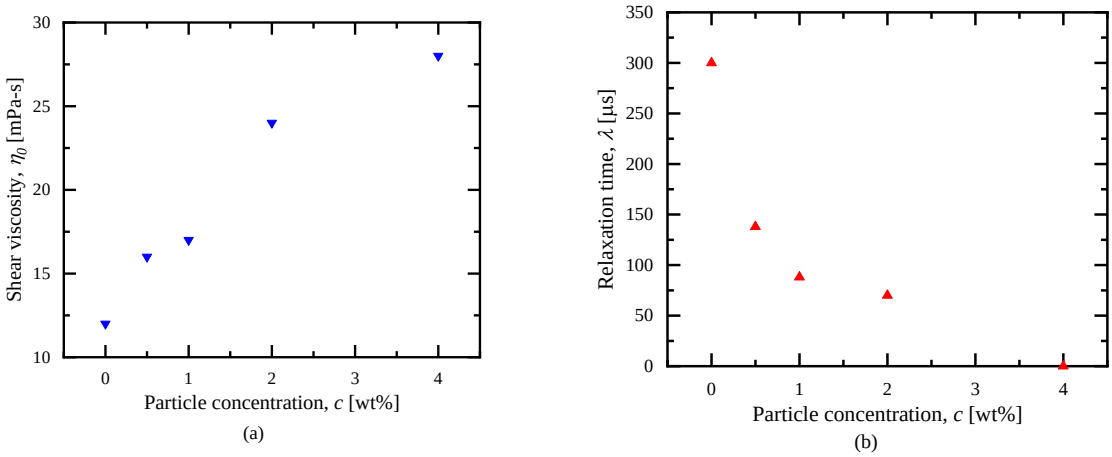

Figure 3.8: (a) Shear viscosity and (b) relaxation time as a function of microparticle concentration obtained from CaBER-DoS experiments

3.6 Particle laden solutions – jetting results

Jetting experiments were performed on the 16 wt% Vinnol E15 with microparticle concentrations of 0 wt%, 0.5 wt%, 1 wt%, 2 wt% and 4 wt%. As reported above, the increase in microparticle concentration caused the solutions to viscosify significantly. As a direct result, the 4 wt% jet was inconsistent and did not provide any measureable data. However, data was obtained for the other cases and the results are presented in Figure 3.8. The main drop volume increased with increase in microparticle concentration which can be attributed to the increased viscosity of the solution. However, one other factor that plays into the increase in main drop volume is the inhomogeneous agglomeration of microparticles in the solution. This inhomogeneity was clearly seen in the CaBER-DoS breakup images, but the effects are also reflected in the main drop volume, where the filaments in between the main drops are not broken up in a continuous, periodic fashion. Rather, the filament breakup occurs in a particle deficient zone, which causes an abrupt retraction of the filament into the main drop. As the microparticle concentration is increased, this effect becomes more pronounced, causing the trend of the main drop volume increasing with increased particle concentration. This effect plays favourably in decreasing the presence of satellite drops, but does not completely eliminate their occurrence. Satellite drop formation and presence in the jet breakup is still possible. In cases where the satellite drop is formed, their behavior is observed and quantified in the satellite drop retraction velocity graph. However, because the effect of elasticity of the Vinnol polymer decreases with increasing particle concentration, the elasticity effects do not significantly affect satellite drop behavior. Satellite drop velocity still decreases as a function of concentration, but increasing the concentration is not conducive to the formation of a periodic jet.

Similarly, breakup time is also affected by the increase in concentration, with the increasing viscosity resisting the growth of the perturbations on the surface of the jet and sustaining the in-between filaments longer. This is a corollary to the results of main drop volume as a function of concentration. Resistance to the growth of perturbations also results in the breakup distance increasing. These results are crucial to the inkjet printing industry as they can use this data to determine the type of binder and microparticle and their potential interaction for each inkjet printing application.

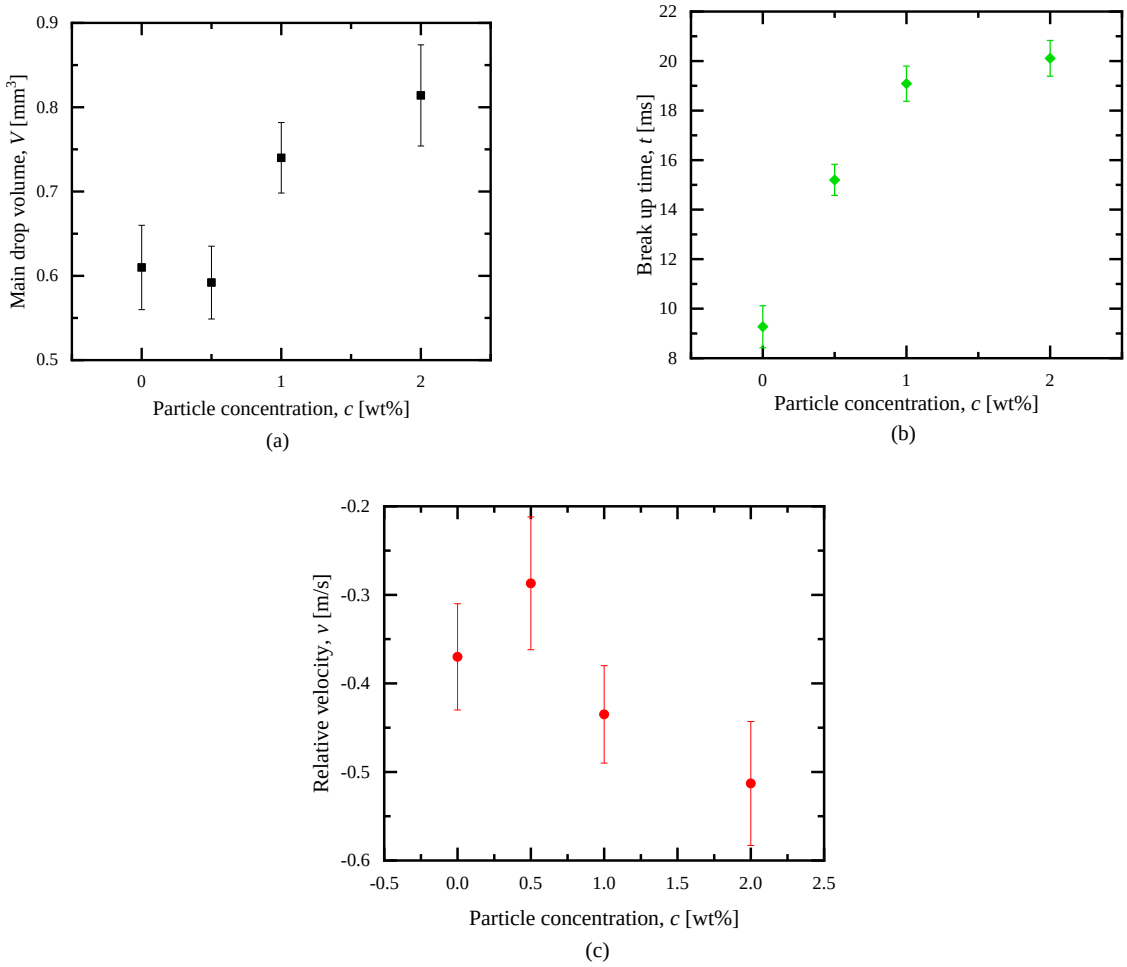

Figure 3.9: (a) Main drop volume trends (b) break up time trends and (c) satellite drop velocity trends as a function of microparticle concentration obtained from jetting experiments

3.7 Particle laden solutions – breakup time analysis

Similar to Section 3.4, breakup time analysis can be performed on the jetting results of the particle laden solutions using the same equations. The results are presented in Figure 3.10. Even adjusting for the jet formation period, it can be seen that even a small amount of microparticles in the fluid greatly influences the jetting behaviour and breakup time of the solutions. High viscosity causes the growth of the perturbations to be slowed down significantly. Not only is the viscosity of the solution increased, the local viscosity in the filament formed in between the drops is also high in the initial stages of the filament breakup. [49,50] This local increase can cause the filament to be reabsorbed back into the jet and thereby increase the breakup time. As this effect is amplified in higher particle concentrations, the experimental results are to be considered with a degree of uncertainty and only lower concentrations of the particles can be reliably used in future experiments. The inhomogeneous distribution of particles can cause localised decreases in viscosity too, where the filament thinning dynamics is entirely reliant on the properties of the polymeric binder. However, as seen in the CaBER results, this localized zone of only polymeric property influence is only present in the final frames of the breakup process, and similarly, are present only for a very short time in the jet breakup process as well. Hence, the results of the final frames of breakup are presented with a degree of error in them. Further experiments and analysis into the distribution of particles along the filament and the viscosity distribution along the filament can help shed further light into the breakup dynamics of particle laden solutions.

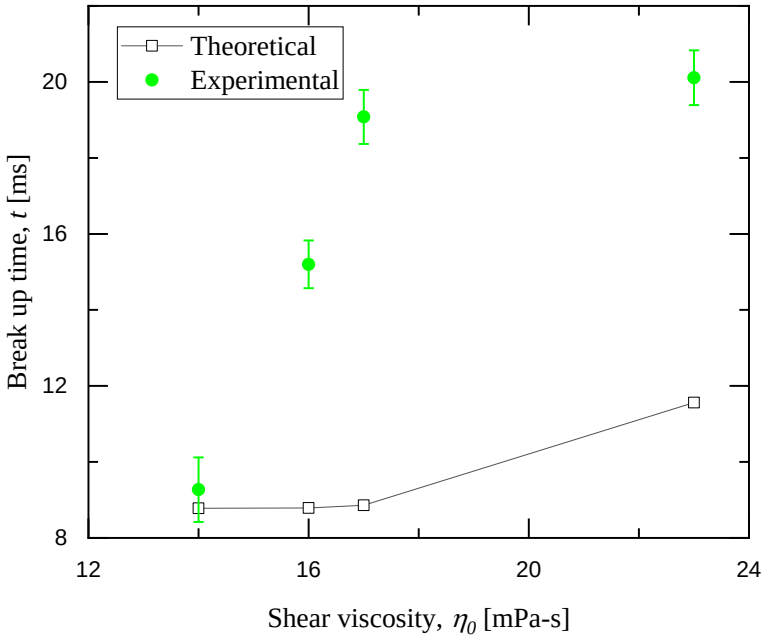

Figure 3.10: Breakup time trends and theoretical breakup time predictions versus shear viscosity for particle laden solutions

CHAPTER 4

CONCLUSIONS

A parametric study was performed on a series of inkjet inks. The inks contained different polymeric binders of varying concentration and molecular weight. These inks had similar behavior in a shear flow, but displayed completely different reactions in extensional flows. The concentration of the polymeric binder was steadily increased until the effects of elasticity became significant in the flow. Jetting studies were performed on the fluids. The first effect of elasticity was seen in the results that showed increased break up time as the concentration of the polymer increased. Similar effects were seen in the jet drop formation as the size of the main jet drop increased and the size of the satellite drop decreased or tapered off to a constant value as the concentration of the polymer was increased. Both these results are also yardsticks to measure the effects of elasticity in the flow. Satellite drop velocity was also measured and was observed to increase negatively as the polymer concentration increased, suggesting that as the polymer concentration increased, the satellite drops both decreased in size and retracted faster back into the jet. Hence, a set of markers were identified to quantify elasticity in weakly viscoelastic solutions through the evaluation of satellite drop behavior. Satellite drop studies were performed in the second part of the study, focusing on the formation and motion of a single satellite drop. High speed imaging revealed that the position of the satellite drop was a linear function of time, and hence travelled with a constant velocity, which resulted in not being able to measure the elastic restoring force acting on the satellite drop. The third part of the study was on the addition of microparticles to the 16 wt% Vinnol E15 solution. While the solution was

elastic with no microparticles added, the elastic effects decreased in magnitude as the concentration of the microparticles increased, disappearing completely at higher concentrations, while the viscosity of the solutions increased correspondingly with increase in concentration. This can be attributed to the adsorption of the polymer molecules onto the surface of the microparticles. Furthermore, the microparticles have a tendency to agglomerate, leading to inhomogeneous regions of particle accumulation. This irregular accumulation causes the filaments in both CaBER-DoS and jetting experiments to breakup in an asymmetric fashion. The effect of such accumulation can be seen in the main drop volume, breakup time and satellite drop retraction velocities.

CHAPTER 5

FUTURE WORK

These experiments leave a lot of scope for future work. Hence, two studies are proposed as follows. The high speed imaging can be used to look at satellite drop formation and motion in polymeric jet systems that are heavily viscoelastic, with relaxation times on the order of milliseconds. As the elasticity effects are more apparent in these systems, the retraction force can be accurately measured using this technique. This can be an excellent addition to the repository of studies that focus studying elastic behaviour of polymeric systems, albeit through other means. The second set of studies can focus on satellite drop formation and behaviour in particle laden solutions. High speed imaging can give more insight into microparticle agglomeration, polymer adsorption, local microparticle concentration inhomogeneity and how these factors affect filament thinning and breakup in jetting systems and can serve as supporting studies to CaBER-DoS experiments.

Bibliography

1. Flory, P. *Principles of polymer processing*. *Ithaca: Cornell University Press* (1953). doi:10.5860/choice.44-2729.
2. Tirtaatmadja, V., Mckinley, G. H. & Cooper-White, J. J. Drop formation and breakup of low viscosity elastic fluids: Effects of molecular weight and concentration ARTICLES YOU MAY BE INTERESTED IN. *Phys. Fluids* **18**, (2006).
3. Plateau, J. Experimental and Theoretical Statics of Liquids subject to Molecular Forces only. *Gauthier-Villars Paris* vol. 1 1863–1866 (1873).
4. Rayleigh, L. On the capillary phenomenon of jets. *Proceedings of the Royal Society of London* vol. 29 71–97 (1879).
5. Rayleigh, L. On the instability of jets.pdf. *Proc. London Math. Soc.* **10**, 4–13 (1878).
6. Eggers, J. Nonlinear dynamics and breakup of free-surface flows. *Rev. Mod. Phys.* **69**, 885–929 (1997).
7. de Gans, B.-J., Duineveld, P. C. & Schubert, U. S. Inkjet Printing of Polymers: State of the Art and Future Developments. *Adv. Mater.* **16**, 203–213 (2004).
8. Basaran, O. A., Gao, H. & Bhat, P. P. Nonstandard Inkjets. *Annu. Rev. Fluid Mech.* **45**, 85–113 (2012).
9. Abe, K., Suzuki, K. & Citterio, D. Inkjet-Printed Microfluidic Multianalyte Chemical Sensing Paper. doi:10.1021/ac800604v.
10. Eom, S. H. *et al.* High efficiency polymer solar cells via sequential inkjet-printing of PEDOT:PSS and P3HT:PCBM inks with additives. (2010)

doi:10.1016/j.orgel.2010.06.007.

11. Gorter, H. *et al.* Toward inkjet printing of small molecule organic light emitting diodes. (2013) doi:10.1016/j.tsf.2013.01.041.

12. Graham D Martin, Stephen D Hoath & Ian M Hutchings. Inkjet printing-the physics of manipulating liquid jets and drops. *J. Phys. Conf. Ser. OPEN ACCESS* **1005**, (2008).

13. Castrejón-Pita, J. R. *et al.* Future, Opportunities and Challenges of Inkjet Technologies. *At. sprays* **23**, 541–565 (2013).

14. Bazilevskii, by, Bazilevskii, A. V, Meyer, J. D. & Rozhkov, A. N. Dynamics and Breakup of Pulse Microjets of Polymeric Liquids. *Fluid Dyn.* **40**, 45–63 (2005).

15. Eggers, J. & Villermaux, E. Physics of liquid jets. *Rep. Prog. Phys.* **71**, 36601 (2008).

16. Clasen, C. *et al.* How dilute are dilute solutions in extensional flows? *J. Rheol. (N. Y. N. Y).* **50**, 881 (2006).

17. Bhat, P. P. *et al.* Formation of beads-on-a-string structures during break-up of viscoelastic filaments. *Nat. Phys.* **6**, 625–631 (2010).

18. Middleman, S. Stability of a viscoelastic jet.pdf. *Chem. Engg. Sci.* **20**, 1037–1040 (1965).

19. Goldin, M., Yerushalmi, J., Pfeffer, R. & Shinnar, R. Breakup of a laminar capillary jet of a viscoelastic fluid.pdf. *J. Fluid Mech.* **38**, 689–711 (1969).

20. Entov, V. M. & Yarin, A. L. Influence of elastic stresses on the capillary breakup of dilute polymer solutions.pdf. *Fluid Dyn.* **19**, 21–29 (1984).

21. Derby, B. Inkjet Printing of Functional and Structural Materials: Fluid Property

Requirements, Feature Stability, and Resolution. *Annu. Rev. Mater. Res.* **40**, 395–414 (2010).

22. Clasen, C., Phillips, P. M., Palangetic, L. & Vermant, and J. Dispensing of rheologically complex fluids: The map of misery. *AIChE J.* **58**, 3242–3255 (2012).

23. Hoath, S. D., Harlen, O. G. & Hutchings, I. M. Jetting behavior of polymer solutions in drop-on-demand inkjet printing. *J. Rheol. (N. Y. N. Y).* **56**, 1127 (2012).

24. Mckinley, G. H. & Sridhar, T. FILAMENT-STRETCHING RHEOMETRY OF COMPLEX FLUIDS. *Annu. Rev. Fluid Mech* 375–415 (2002).

25. Anna, S. L. & Mckinley, G. H. Elasto-capillary thinning and breakup of model elastic liquids. *Cit. J. Rheol.* **45**, 138 (2001).

26. Vadillo, D. C., Mathues, W. & Clasen, C. Microsecond relaxation processes in shear and extensional flows of weakly elastic polymer solutions. *Rheol. Acta* **51**, 755–769 (2012).

27. Dinic, J., Nallely Jimenez, L. & Sharma, V. Pinch-off dynamics and dripping-onto-substrate (DoS) rheometry of complex fluids. *Lab Chip* **17**, 473 (2017).

28. Dinic, J., Zhang, Y., Jimenez, N. & Sharma, V. Extensional Relaxation Times of Dilute, Aqueous Polymer Solutions. *ACS Macro Lett.* **4**, 804–808 (2015).

29. Sur, S. & Rothstein, J. Drop breakup dynamics of dilute polymer solutions: Effect of molecular weight, concentration, and viscosity. *J. Rheol. (N. Y. N. Y).* **62**, 1245 (2018).

30. de Gans, B.-J., Kazancioglu, E., Meyer, W. & Schubert, U. S. Ink-jet Printing Polymers and Polymer Libraries Using Micropipettes. *Macromol. Rapid Commun.*

25, 292–296 (2004).

31. Shore, H. J. & Harrison, G. M. The effect of added polymers on the formation of drops ejected from a nozzle. *Phys. Fluids* **17**, 33104 (2005).

32. Christanti, Y. & Walker, L. M. Effect of fluid relaxation time of dilute polymer solutions on jet breakup due to a forced disturbance. *J. Rheol. (N. Y. N. Y).* **46**, 748 (2002).

33. Christanti, Y. & Walker, L. M. Surface tension driven jet break up of strain-hardening polymer solutions. *J. Non-Newtonian Fluid Mech* **100**, 9–26 (2001).

34. Vadillo, D. C. *et al.* Evaluation of the inkjet fluid's performance using the "Cambridge Trimaster" filament stretch and break-up device. *J. Rheol. (N. Y. N. Y).* **54**, 261–282 (2010).

35. Rosello, M., Sur, S., Barbet, B. & Rothstein, J. P. Dripping-onto-substrate capillary breakup extensional rheometry of low-viscosity printing inks. *J. Nonnewton. Fluid Mech.* **266**, 160–170 (2019).

36. Donnelly, R. J. & Glaberson, W. Experiments on the capillary instability of a liquid jet. *," Proc. R. Soc. London Ser. A, Math. Phys. Sci.* 547–556 (1965).

37. Keller, J. B. & Miksis, M. J. Surface Tension Driven Flows. *SIAM J. Appl. Math.* **43**, 268–277 (1983).

38. Campo-Deaño, L. & Clasen, C. The slow retraction method (SRM) for the determination of ultra-short relaxation times in capillary breakup extensional rheometry experiments. *J. Nonnewton. Fluid Mech.* **165**, 1688–1699 (2010).

39. McKinley, G. H. Visco-elasto-capillary thinning and break-up of complex fluids. *Rheol. Rev.* **3**, 1–48 (2005).

40. Papageorgiou, D. T. On the breakup of viscous liquid threads. *Phys. Fluids.* **7**, 1529–1544 (1995).

41. Amarouchene, Y., Bonn, D., Meunier, J. & Kellay, H. Inhibition of the Finite-Time Singularity during Droplet Fission of a Polymeric Fluid. *Phys. Rev. Lett.* **86**, 3558–3561 (2001).

42. Brandrup, J. & Immergut, E. H. *Polymer Handbook*. (John Wiley & Sons, 1989).

43. Hoath, S. D. *et al.* Inkjet printing of weakly elastic polymer solutions. *J. Nonnewton. Fluid Mech.* **205**, 1–10 (2014).

44. Morrison, N. F. & Oliver Harlen. VISCOELASTICITY IN INKJET PRINTING. *Rheol. Acta* **49**, 619–632 (2010).

45. Ng, S. L., Mun, R. P., Boger ~', D. V & James, D. F. Extensional viscosity measurements of dilute solutions of various polymers. *J. Non-Newtonian Fluid Mech* **65**, 291–298 (1996).

46. Zyła, G. ˙ & Fal, J. Viscosity, thermal and electrical conductivity of silicon dioxide-ethylene glycol transparent nanofluids: An experimental studies. *Thermochim. Acta* **650**, 106–113 (2017).

47. Shakesheff, K. M., Evora, C., Soriano, I. & Langer, R. The Adsorption of Poly(vinyl alcohol) to Biodegradable Microparticles Studied by X-Ray Photoelectron Spectroscopy (XPS). *J. Colloid Interface Sci.* **185**, 538–547 (1997).

48. Bertrand, T., Bonnoit, C., Clément, E. & Lindner, A. Dynamics of drop formation in granular suspensions: The role of volume fraction. *Granul. Matter* **14**, 169–174 (2012).

49. Mathues, W., Mcilroy, C., Harlen, O. G. & Clasen, C. Capillary breakup of

suspensions near pinch-off. *Phys. Fluids* **27**, 93301 (2015).

50. Lindner, A., Fiscina, J. E. & Wagner, C. Single particles accelerate final stages of capillary break up. *Europhys. Lett.* **110**, (2015).